Environmental Science & Technology

Article

pubs.acs.org/est

Kinetics and Mechanism of •OH Mediated Degradation of Dimethyl Phthalate in Aqueous Solution: Experimental and Theoretical Studies

Taicheng An,[†,*] Yanpeng Gao,[†,‡] Guiying Li,[†] Prashant V. Kamat,[§,∥,*] Julie Peller,[⊥] and Michelle V. Joyce[∥]

[†]State Key Laboratory of Organic Geochemistry, Guangzhou Institute of Geochemistry, Chinese Academy of Sciences, Guangzhou 510640, People's Republic of China

[‡]University of Chinese Academy of Sciences, Beijing 100049, People's Republic of China

[§]Radiation Laboratory and [∥]Department of Chemistry and Biochemistry, University of Notre Dame, Notre Dame, Indiana 46556

[⊥]Department of Chemistry, Indiana University-Northwest, Gary, Indiana 46408, United States

Supporting Information

ABSTRACT: The hydroxyl radical (•OH) is one of the main oxidative species in aqueous phase advanced oxidation processes, and its initial reactions with organic pollutants are important to understand the transformation and fate of organics in water environments. Insights into the kinetics and mechanism of •OH mediated degradation of the model environmental endocrine disruptor, dimethyl phthalate (DMP), have been obtained using radiolysis experiments and computational methods. The bimolecular rate constant for the •OH reaction with DMP was determined to be $(3.2 \pm 0.1) \times 10^9$ $M^{-1}s^{-1}$. The possible reaction mechanisms of radical adduct formation (RAF), hydrogen atom transfer (HAT), and single electron transfer (SET) were considered. By comparing the experimental absorption spectra with the computational results, it was concluded that the RAF and HAT were the dominant reaction pathways, and OH-adducts (•$DMPOH_1$, •$DMPOH_2$) and methyl type radicals •DMP(-H)α were identified as dominated intermediates. Computational results confirmed the identification of transient species with maximum absorption around 260 nm as •$DMPOH_1$ and •DMP(-H)α, and these radical intermediates then converted to monohydroxylated dimethyl phthalates and monomethyl phthalates. Experimental and computational analyses which elucidated the mechanism of •OH-mediated degradation of DMP are discussed in detail.

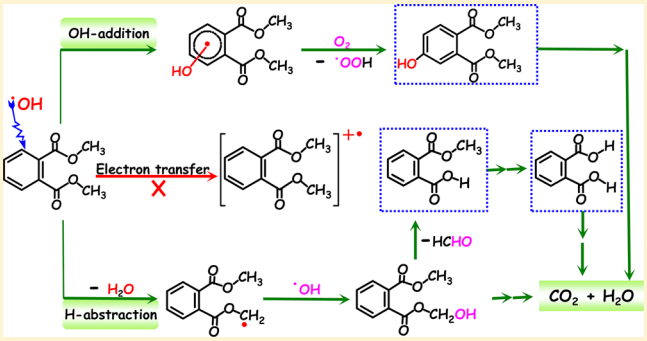

INTRODUCTION

In recent years, advanced oxidation processes (AOPs), defined by highly reactive species, predominantly hydroxyl radicals (•OH), have become attractive alternatives to various conventional environmental remediations, especially in the field of wastewater treatment. In aqueous systems, a number of AOPs, such as photocatalysis,[1] Fenton's reaction,[2,3] ozone-based oxidation,[4] UV−H_2O_2 [5] and radiolysis,[6] have been successfully employed to degrade organic pollutants.[7−9] The mechanisms of complete oxidation are often complex and involve several reaction steps. Many studies have reported that the initial step of the •OH-initiated reaction of organics is followed by a radical molecular mechanism, which is not energetically favored,[10,11] and not competitive with the subsequent radical−radical coupling reactions. Thus, the initial step of •OH-mediated degradation of organic pollutants is crucial to determine the subsequent reactions and fates of organics in water. Degradation products are also very important, and may be more environmentally problematic.[12,13] Therefore, a fundamental understanding of the fate and transformation by-products of organic pollutants in AOPs systems, including the detailed mechanisms and kinetics of the •OH-mediated degradation of organics, is important to effectively improve the application AOPs in wastewater treatment.

It is well-known that •OH is a highly reactive species with an oxidation potential of 2.8 V.[14] It can oxidize organics in aqueous medium via three possible reaction mechanisms, e.g., •OH addition to an aromatic ring or other unsaturated bond leading to the radical adduct formation (RAF, eq 1), hydrogen atom transfer by •OH (HAT, eq 2), and/or single electron transfer with •OH (SET, eq 3).[15,16]

$$\text{RAF: } A + {}^{\bullet}OH \rightarrow {}^{\bullet}AOH \quad (1)$$

$$\text{HAT: } A + {}^{\bullet}OH \rightarrow {}^{\bullet}A(-H) + H_2O \quad (2)$$

$$\text{SET: } A + {}^{\bullet}OOH \rightarrow A^{\bullet+} + OH^- \quad (3)$$

Received: October 5, 2013
Revised: December 9, 2013
Accepted: December 10, 2013
Published: December 10, 2013

In the commonly held RAF mechanism, the •OH can easily react with aromatic molecules such as benzene, benzaldehydes, quinoline, and sulfa drugs by addition to the benzene ring, producing OH-adducts.[17−20] Most experimental investigations have focused only on their characteristic absorptions around 310−410 nm, and the absorption below 290 nm has received limited attention. As a result, some important mechanistic information of these •OH reactions is likely to be neglected. For instance, Sehested et al. found that besides the addition of •OH to the benzene ring of methylated benzenes, •OH could also abstract a hydrogen atom to form methylbenzyl radicals,[21] characterized by absorption in the 260−270 nm range. This HAT mechanism was also confirmed by the work of Song et al.,[22] where more than 50 of such active sites within microcystin-LR can react with •OH via the HAT reaction. Conversely, the •OH reactions with furazan derivatives to form aniline radicals with an absorption peak at 290 nm, occur by the RAF mechanism and further dehydration, rather than the HAT mechanism.[23] Thus, careful experimental studies must be conducted to distinguish RAF mechanism from HAT mechanism.

Due to the similar absorption spectra generated by •OH-adducts and cation radicals as claimed previously, limited experimental information has been reported on the SET mechanism of •OH reactions,[17,24] although the SET mechanism has been considered as a dominant pathway for •OH-mediated reactions of some aromatic molecules.[25,26] The lifetime of cation radicals formed through the SET mechanism was extremely short, and the cation radicals hydrolyzed to form OH-adducts in aqueous medium. As a result, it is often difficult to experimentally distinguish the RAF mechanism from the SET mechanism in •OH-mediated reactions.

Quantum chemical calculations have proven to be a powerful tool to obtain deeper insight into reaction mechanisms and kinetics, as well as offer a very valuable complement to experimental studies.[27,28] Unfortunately, only a few theoretical studies can be found on the •OH-mediated degradation mechanisms of organic pollutants in AOPs. For example, Nicolaescu et al. successfully investigated the RAF mechanism of the •OH-mediated degradation of quinolone.[29] A comprehensive study can be very useful for understanding the transformation mechanisms of organics in wastewater treatment using AOPs.

In this study, both radiolysis experiments and quantum chemical calculations were employed to elucidate the mechanisms of •OH-mediated degradation of dimethyl phthalate (DMP). DMP, the simplest phthalate, is of particular interest since it is a widely prevalent, relatively simple, aromatic contaminant, and an endocrine-disrupting chemical.[30,31] The reactions of DMP with various oxidative radicals, such as •OH, azide radicals ($^{\bullet}N_3$) as well as sulfate radicals ($SO_4^{\bullet-}$), produced by pulse radiolysis, were investigated comparatively. Moreover, the intermediates formed in the steady-state radiolysis were identified by HPLC-MS-MS and doubly confirmed with authentic standards. Additionally, the quantum chemical calculations, as well as the theoretical determinations of transition spectra of possible intermediate radicals, were carried out to thoroughly comprehend the •OH-mediated degradation mechanisms of DMP in aqueous phase AOPs.

EXPERIMENTAL SECTION

Chemicals and Reagents. Dimethyl phthalate (DMP, >98% purity), phthalic acid (PA, >98%) and monomethyl phthalate (MMP, >97%) were purchased from Sigma-Aldrich and dimethyl 4-hydroxylphthalate (*m*-DMPOH, >98%) was obtained from Tokyo Chemical Industry. All irradiation solutions were prepared using high purity deionized water (Millipore Corp., 18 MΩ cm), which included constant illumination by a Xe arc lamp at 172 nm to keep total organic carbon concentrations below 13 μg L^{-1}. The solutions used in the radiolysis experiments were prepared with buffer and adjusted to pH 7.0 and sparged with high-purity N_2O (for •OH and $^{\bullet}N_3$ experiments) or N_2 (for $SO_4^{\bullet-}$ experiments) to remove dissolved oxygen.

Radiolysis Experiments. Electron pulse radiolysis experiments were performed at the Notre Dame Radiation Laboratory using the 8-MeV Titan Beta model TBS-8/16-1S linear accelerator with pulse lengths of 2.5−10 ns. This irradiation and transient absorption detection system has been described previously in detail.[1] Dosimetry was carried out using N_2O-saturated of 10 mM potassium thiocyanate (KSCN) solutions as described elsewhere.[19,32] All experimental data were determined by averaging 8−12 replicate pulses using the continuous flow mode of the instrument. The radiolysis of water is described in eq 4, where the numbers in parentheses are the *G*-values (yields) in μmol J^{-1}.[33,34]

$$H_2O \rightarrow {}^{\bullet}OH(0.28) + e_{aq}^{-}(0.27) + {}^{\bullet}H(0.06) + H_2(0.05) + H_2O_2(0.07) + H^{+}(0.27) \quad (4)$$

A Shepherd 109-86 Cobalt 60 (^{60}Co) γ source was used for steady-state γ radiolysis experiments with a dose rate of 1.82 krad min^{-1}, as measured by Fricke dosimetry. For only oxidative conditions, all aqueous solutions were presaturated with N_2O before γ-irradiation.

HPLC Analysis. Concentrations of DMP were analyzed using a model 2669 Waters high performance liquid chromatography (HPLC) coupled with a PDA detector and a reverse phase Hypersil BDS C18 column (150 mm × 4.6 mm, 3 μm) column. The injection volume was 20 μL, and the mobile phase was composed of acetonitrile/water (70:30) with a flow rate of 0.6 mL min^{-1}. Identification and qualification of degradation intermediates were performed with a Waters HPLC-MS-MS (ABI API 3000 System), and further confirmed by the comparison of the retention times and spectra of authentic samples using HPLC.

Computational Methods. All of the electronic structure calculations were carried out with the Gaussian 03 program,[35] and the equilibrium geometries and frequencies of the stationary points (reactants, products, transition states, and intermediates) were calculated at the B3LYP/6-31G(d,p) levels. Vibrational frequency calculations were used to identify all of the stationary points as either minima (zero imaginary frequency) or transition states (one imaginary frequency). The minimum-energy path (MEP) was constructed with the intrinsic reaction coordinate (IRC) theory at the same levels to confirm that the transition state corresponded with minima along the reaction pathways. Single point calculations were performed at the B3LYP/6-311++G(d,p) on the optimized structures, and the solvent effect was also considered by single-point calculations using the conductive polarizable continuum model (CPCM),[29,36] with a dielectric constant of 78.39 for water.[37] Using the same approach, full optimization in aqueous solution was carried out for the most representative pathway. In both cases, the results and geometries confirm the trend observed with gas-phase structures calculations (discussed in

the Supporting Information, SI). The absorption spectra were modeled with time-dependent density function theory (TDDFT) at the B3LYP/6-311++G(d,p) level. All energies are in kcal/mol, and all bond lengths are in angstroms, unless otherwise specified, and all computations were done at 298.15 K and 1 atm.

RESULTS AND DISCUSSION

Pulse Radiolysis Studies. To study the reaction of $^{\bullet}OH$ with DMP, solutions were presaturated with N_2O, which quantitatively converts the hydrated electrons and hydrogen atoms to $^{\bullet}OH$ radicals under pulse irradiation conditions, as described elsewhere.[38] Using a DMP solution, the time-resolved transient absorption spectra of $^{\bullet}OH$ + DMP were generated and recorded (Figure 1a). Three characteristic peaks

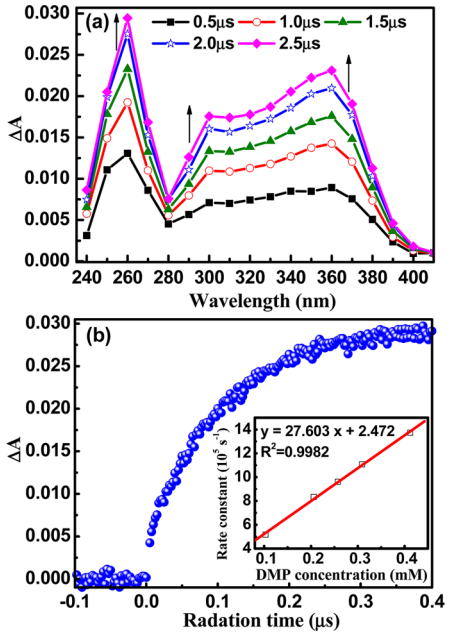

Figure 1. (a) Time-resolved transient absorption spectra recorded during the reaction of $^{\bullet}OH$ with DMP (0.26 mM and pH 7) at room temperature for different times. (b) The build-up at 260 nm during the pulse radiolysis of a solution of DMP with concentration of 50 mM in N_2O-saturated pH 7.0 solution. Inset: plot of the first-order transient formation rate constant at 260 nm vs different DMP concentrations in the reaction with $^{\bullet}OH$ radical.

at 260, 300, and 360 nm were observed. According to the similar spectra from the reaction of $^{\bullet}OH$ with several structural analogs,[21,39,40] the maximum absorption at 260 nm can be attributed tentatively to the methylene type radical ($^{\bullet}$DMP(-H)α), formed by the HAT mechanism from the methyl group of DMP. In addition, this transient species was formed and increased within the short lifetime scale of 2.5 μs, followed by a rapid decay. The typical growth kinetic curve of the transient radicals is plotted in Figure 1b. The bimolecular rate constant for the $^{\bullet}OH$ reaction with DMP was determined as $(3.2 \pm 0.1) \times 10^9$ $M^{-1}s^{-1}$ from the linear dependence of the first-order growth rate constant on the DMP concentration (see insert in Figure 1b). Moreover, this rate constant was the same order of magnitude as previously reported values: $(2.67 \pm 0.26) \times 10^9$ $M^{-1}s^{-1}$ using the competition kinetics method,[41] and 3.4×10^9 $M^{-1}s^{-1}$ using pulse radiolysis experiments,[6] as well as 4.0×10^9 $M^{-1}s^{-1}$ through fitting the experimental data to the kinetic model.[42]

The absorption peaks in the region 300−360 nm correspond to $^{\bullet}OH$-adducts of DMP according to pulse radiolysis studies by Wu et al.,[6] but the formation of the adducts from the cation radical ($DMP^{+\bullet}$) should not be neglected since both intermediates exhibit similar absorption in this region.[19] Thus, additional experimentation is needed to distinguish these transient intermediates and estimate the contribution of the RAF and SET mechanisms to the $^{\bullet}OH$-mediated degradation of DMP.

To determine the contribution of the SET mechanism of $^{\bullet}OH$, the reaction of DMP with $^{\bullet}N_3$ was investigated. The $^{\bullet}N_3$, a milder and more selective species than $^{\bullet}OH$, can exclusively participate in SET reaction via primary formation of radical cations.[43] Azide radicals are generated by pulse radiolysis of N_2O-saturated sodium azide solutions as described in eq 5.[44]

$$^{\bullet}OH + N_3^- \rightarrow OH^- + {}^{\bullet}N_3 \quad k_4 = 1.2 \times 10^{10} M^{-1}s^{-1} \tag{5}$$

An N_2O-saturated solution containing 10 mM NaN_3 and 0.26 mM DMP mixture was used to investigate the reaction of $^{\bullet}N_3$ with DMP at different time intervals. The transient absorption spectra showed very weak absorption in the 300−360 nm regions (Figure 2a), in addition to the characteristic

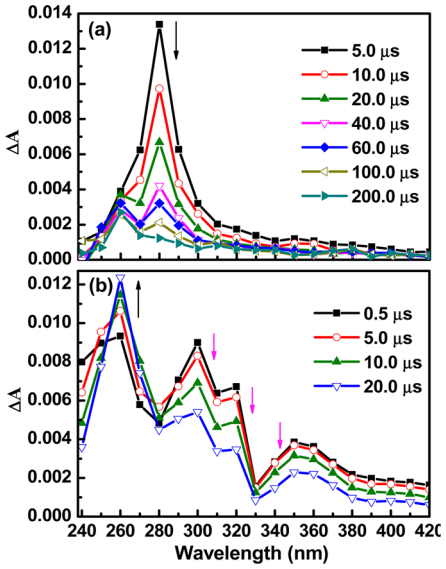

Figure 2. Time-resolved transient absorption spectra recorded at room temperature for different time intervals during the reaction between DMP (0.26 mM and pH 7) and (a) $^{\bullet}N_3$; (b) $SO_4^{\bullet-}$.

absorption peak of the $^{\bullet}N_3$ around ~280 nm.[45] The absorption intensity in the 300−360 nm range was only a tenth of that observed in the $^{\bullet}OH$ radical reaction within the irradiation time at 5 μs. This is due to the low reactivity of $^{\bullet}N_3$ with oxidation potential (E^0 = 1.33 V vs NHE).[46] Therefore, an additional experiment was required to clarify the contribution of the SET mechanism in the $^{\bullet}OH$-mediated degradation of DMP.

The sulfate radical anion is a stronger oxidant ($SO_4^{\bullet-}$, E^0 = 2.43 V vs NHE)[47] which can also undergo SET reactions with organics. The $SO_4^{\bullet-}$ is formed in N_2-saturated solutions containing $K_2S_2O_8$ (5 mM) and *tert*-butyl alcohol (50 mM) as described in eq 6,[48] with the yield of G ($SO_4^{\bullet-}$) = 2.7 μmol J^{-1}:

dx.doi.org/10.1021/es404453v | Environ. Sci. Technol. 2014, 48, 641−648

$$S_2O_8^{2-} + e^-_{aq} \rightarrow SO_4^{2-} + SO_4^{\bullet-}$$
$$k_5 = 1.1 \times 10^{10} M^{-1}s^{-1} \quad (6)$$

The transient absorbance spectra obtained for the reaction of $SO_4^{\bullet-}$ with DMP are shown in Figure 2b. A strong absorption was generated at 260 nm, similar to those obtained from the $^{\bullet}OH$ or $^{\bullet}N_3$ reaction with DMP. As mentioned above, the transient intermediate at 260 nm also is likely ascribed to the methyl benzyl radical ($^{\bullet}DMP(-H)\alpha$). In addition, from Figure 2b, it is interesting to note that the shape of the spectrum above 300 nm was different from that of the $^{\bullet}OH$ reactions. Along with the decrease of the absorbance around 300−360 nm, a new transient peak with the absorption spectrum at 260 nm was formed and increased with the increase of radiation time during the reaction of $SO_4^{\bullet-}$ with DMP. This result could provide the evidence that the radical cations ($DMP^{\bullet+}$) with the absorption in the 300−360 nm region could be initially generated in the SET reaction of $SO_4^{\bullet-}$ with DMP. Then, the short-lived $DMP^{\bullet+}$ rapidly decays, leading to the formation of the methylene type radicals ($^{\bullet}DMP(-H)\alpha$) at 260 nm.[49] Due to the different spectra shape at 300−360 nm, it may be deduced that $DMP^{\bullet+}$ is unlikely to be formed in the $^{\bullet}OH$-mediated reaction. However, the spectral information obtained herein only detected transient intermediates which seemed to overlap with that in the $^{\bullet}OH$ reactions. Therefore, it is difficult to fully distinguish the origin of the intermediates resulting from different mechanisms in the studied time scale. Thus, the detailed quantum chemical calculations of transient absorbance spectra of some intermediate radicals will aid in the confirmation of the experimentally determined intermediates.

Identification of Degradation Products and Assignment of Transient Spectra. Steady-state radiolysis experiments of DMP in N_2O saturated solution were performed using a ^{60}Co γ source to identify the stable intermediates formed in the reactions of $^{\bullet}OH$-mediated oxidation of DMP. A representative HPLC chromatogram of the products formed during the γ-radiolysis of N_2O-saturated solution of DMP is depicted in Figure 3a. On the basis of the retention time (t_R) and spectrum of authentic standards, four stable degradation products, phthalic acid (PA) (t_R = 1.80 min), monomethyl phthalate (MMP) (t_R = 3.61 min), meta-hydroxylated DMP (*m*-OH-DMP) (t_R = 4.25 min), and ortho-hydroxylated DMP (*o*-OH-DMP) (t_R = 4.57 min), were identified by HPLC-MS-MS. The decay of DMP during this process as a function of the irradiation dose, together with the evolution of degradation products, are also illustrated in Figure 3b. Within 90 min of γ-irradiation, corresponding to an irradiation dose of 1.64 kGy, 92.0% of DMP was degraded. By fitting the decay to single exponential decay kinetics, the half-life for the degradation of DMP under these conditions (with dose rate of 1.82 krad min^{-1}) was calculated to be ~44.2 min. Furthermore, with the gradual decrease of DMP concentration, the concentrations of all intermediates exhibited similar changing trends except for PA. The three main intermediates first increased dramatically and then decreased swiftly with further increase of radiation dose. That is, the maximum concentrations were 19.77 mM for *m*-OH-DMP at 50 min, 8.16 mM for *o*-OH-DMP at 30 min, and 22.19 mM for MAP at 10 min, respectively. However, the concentration of PA was always relatively low (less than 0.50 mM) until 90 min, suggesting that it was a secondary product of DMP degradation. Of course, DMP and its degraded products will be oxidized further into CO_2 and H_2O with further extension of the degradation time over 90 min.

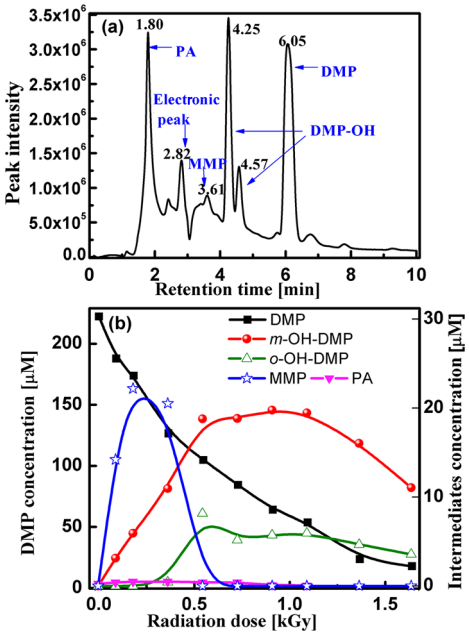

Figure 3. (a) HPLC chromatogram of degradation products obtained from the γ-radiolysis degradation of the DMP. (b) Concentration profiles of DMP and degradation products during γ-radiolysis of DMP with an initial concentration of 0.25 mM.

Three primary products (*m*-OH-DMP, *o*-OH-DMP, and MMP), confirmed experimentally with the authentic standards, can be correlated with several transient intermediates: OH-adducts ($^{\bullet}DMP\text{-}OH_1$ and $^{\bullet}DMP\text{-}OH_2$), carbon centered radical ($^{\bullet}DMP(-H)\alpha$) and/or $DMP^{\bullet+}$. Computational methods were employed to further validate and explore these species. First, the reliability of the method was confirmed by calculating the absorption spectra of the hydroxycyclohexadienyl radical ($C_6H_6OH^{\bullet}$) as shown in SI Figure S1. The maximum absorption around 310 nm was well in agreement with a previous experimental value (315 nm).[50] Thus, the transition spectra of these potential intermediate radicals, $^{\bullet}DMPOH_1$, $^{\bullet}DMPOH_2$, $^{\bullet}DMP(-H)\alpha$), and $DMP^{\bullet+}$ were modeled at the same level and compared with the experimental spectra of the $^{\bullet}OH$-mediated reaction of DMP (SI Figures S2−S5). It is apparent from these spectra that $^{\bullet}DMPOH_1$ and $^{\bullet}DMP(-H)\alpha$ have a maximum absorption at 260 nm, and the transient absorption in the region 300−360 nm were present in the calculated absorption of all transient species, except $^{\bullet}DMP(-H)\alpha$. These results indicate that these four transient species, if formed, would possibly overlap the absorption at these regions. In SI Figure S5, $DMP^{\bullet+}$ exhibits a similar spectral shape as seen with the $SO_4^{\bullet-}$ reaction, and has a maximum absorption at 750 nm, which was not observed in experimental spectra recorded in the $^{\bullet}OH$ reaction. This result confirms that $DMP^{\bullet+}$ could not be formed by the SET mechanism in the $^{\bullet}OH$-mediated reaction of DMP. Therefore, it can be deduced that RAF and HAT mechanisms are likely to be favored in DMP degradation by $^{\bullet}OH$, to produce OH-adducts ($^{\bullet}DMPOH_1$, $^{\bullet}DMPOH_2$) and methyl type radicals ($^{\bullet}DMP(-H)\alpha$), respectively. Furthermore, these transient species could be rapidly converted to the more readily detectable intermediates (*m*-OH-DMP, *o*-OH-DMP, and MMP).

dx.doi.org/10.1021/es404453v | Environ. Sci. Technol. 2014, 48, 641−648

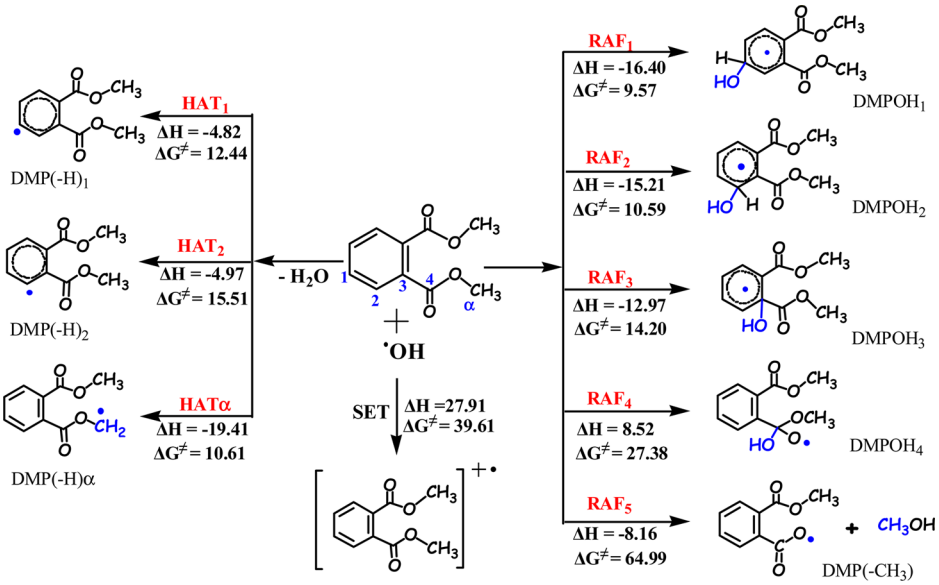

Figure 4. Reaction enthalpies (ΔH) and free energy barriers ($\Delta G^{\ddagger}$) of all possible pathways for the reaction of DMP with •OH. Units of ΔH and $\Delta G^{\ddagger}$ are kcal mol^{-1}.

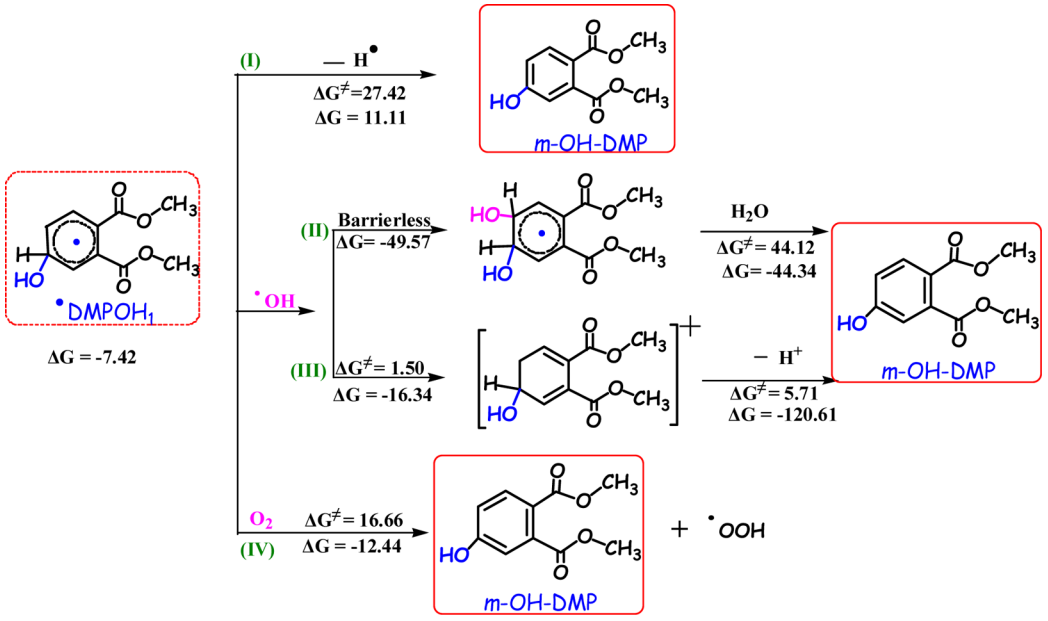

Figure 5. *m*-OH-DMP formation pathways embedded with reaction enthalpies (ΔH) and free energy barriers ($\Delta G^{\ddagger}$). Units of ΔH and $\Delta G^{\ddagger}$ are kcal mol^{-1}.

Reaction Mechanism Calculations. From the experimental data, it can be concluded that DMP is quickly degraded by •OH to form four major products. According to both experimental and computational spectral data, the SET mechanism is insignificant in the •OH-mediated degradation of DMP. However, for RAF and HAT mechanisms, several potential reaction sites exist on the benzene ring and side chains of DMP. To determine the predominant mechanisms and reaction sites of •OH reaction, quantum chemical calculations were performed. All three mechanisms were considered in the theoretical investigation: RAF, HAT, and SET, and all possible reaction pathways of •OH with DMP are depicted in Figure 4. The optimized geometries of the reactant, the formed intermediates and transition states (TS) involved in these pathways are shown in SI Figures S6–S7 and the calculated frequencies of these species are listed in SI Table S1. From SI Figure S6 and Table S1, it can be seen that the calculated geometries and frequencies agreed very well with the available experimental results within 5% at the B3LYP/6-31G(d,p) level.

As shown in Figure 4, on the basis of the reaction enthalpies (ΔH) and energy barriers ($\Delta G^{\ddagger}$) for the different pathways of DMP reaction with •OH, the SET pathway is the most difficult pathway due to high endothermic energy of 27.91 kcal mol^{-1}. While all the RAF and HAT pathways are exothermic processes with ΔH values in the range of −19.41 to −4.97 kcal mol^{-1}, except RAF_4 with a ΔH of 8.52 kcal mol^{-1}. Thus, from the viewpoint of thermodynamics, the SET mechanism can be ruled out as the initial step of •OH reaction with DMP in comparison with the HAT and RAF mechanisms, in agreement

dx.doi.org/10.1021/es404453v | Environ. Sci. Technol. 2014, 48, 641−648

with the experimental data. Therefore, the absorption peak in the region 300−360 nm was assigned to the OH-adducts of DMP and not the radical cations ($DMP^{+\bullet}$) in the •OH-mediated degradation of DMP.

As shown in Figure 4, $\Delta G^{\ddagger}$ values for •OH-addition pathways on the side chains (RAF_4 and RAF_5) were higher by 13.18 to 55.42 kcal mol^{-1} in comparison to benzene •OH-addition pathways (RAF_1, RAF_2, and RAF_3), indicating that •OH addition to the carbonyl of DMP (RAF_4) was an insignificant pathway as well as the demethylation reaction (RAF_5). For the benzene •OH-addition pathways, $\Delta G^{\ddagger}$ values were 9.57, 10.59, and 14.20 kcal mol^{-1} for meta-position addition (RAF_1), ortho-position addition (RAF_2), and ipso-position addition (RAF_3), respectively. It can be seen that $\Delta G^{\ddagger}$ of the latter pathway was higher than those of the former two pathways by 4.63 and 3.61 kcal mol^{-1}, respectively, indicating that RAF_1 and RAF_2 pathways were more likely to occur among these RAF pathways, to mainly produce OH-adducts, $^{\bullet}DMPOH_1$ and $^{\bullet}DMPOH_2$.

In the case of HAT pathways, the $\Delta G^{\ddagger}$ value for the methyl hydrogen transfer pathway (HATα) was 10.61 kcal mol^{-1}, which was lower than those of the benzene hydrogen transfer pathways (HAT_1 and HAT_2) by 1.83 and 4.90 kcal mol^{-1}, respectively. In addition, the ΔH of the former pathway was −19.41 kcal mol^{-1}, which was at least 15 kcal mol^{-1} lower than those of the latter two pathways. As expected, the H atom transfer from the methyl group is more likely than those from the benzene ring, and thus the dehydrogenation radical ($^{\bullet}DMP(-H)\alpha$) was mainly formed.

According to both thermodynamic and kinetic considerations of these processes, •OH additions to the aromatic ring (RAF_1 and RAF_2) and hydrogen atom transfer from a methyl group (HATα) were very feasible. Thus, •OH-adducts ($^{\bullet}DMPOH_1$ and $^{\bullet}DMPOH_2$) and dehydrogenation radicals ($^{\bullet}DMP(-H)\alpha$) are formed in the initial step of the •OH reaction with DMP, consistent with the experimental absorption spectra discussed above. Furthermore, these intermediates can be transformed into the stable products *m*-OH-DMP, *o*-OH-DMP, MMP, and PA. To understand the subsequent transformation reactions in AOPs systems, it is essential to track the stable intermediates formed from $^{\bullet}DMPOH_1$, $^{\bullet}DMPOH_2$, and $^{\bullet}DMP(-H)\alpha$. As $^{\bullet}DMPOH_1$ and $^{\bullet}DMPOH_2$ are structurally similar, $^{\bullet}DMPOH_1$ was selected in the computations example of subsequent reactions so as to decrease the computational cost.

Fate of $^{\bullet}DMPOH_1$ Radical. The subsequent reactions of $^{\bullet}DMPOH_1$ are depicted in Figure 5. From pathway (I), the direct dehydrogenation is unlikely to occur in an aqueous environment, due to high energy barrier of 27.42 kcal mol^{-1}. However, because •OH is continuously generated in this system, another •OH can attack the aromatic ring of $^{\bullet}DMPOH_1$ (pathway (II)), via a barrierless radical−radical reaction with exothermic energy of −49.57 kcal mol^{-1}. And then, monohydroxylated DMP (*m*-OH-DMP) should be rapidly produced, since the high released energy of −49.57 kcal mol^{-1} could completely overcome the energy barrier ($\Delta G^{\ddagger}$= 44.12 kcal/mol) of the subsequent dehydration step. In addition, the single electron transfer from $^{\bullet}DMPOH_1$ (pathway (III)), could also take place through a very small energy barrier ($\Delta G^{\ddagger}$ = 1.50 kcal mol^{-1}). Then the formed short-lived cation might undergo loss of a hydrogen ion to yield *m*-OH-DMP (pathway (III), due to the low energy barrier of 5.71 kcal mol^{-1}. Therefore, for the subsequent reaction of $^{\bullet}DMPOH_1$, both •OH addition and SET reaction might be the feasible pathways for the formation of *m*-OH-DMP.

In the present study, the gamma degradation experiments were carried out in N_2O saturated solution and in the absence of O_2. However, most of AOPs such as photocatalytic degradation[51] and Fenton reaction[52] are often carried out in aerated aquatic environments, indicating that O_2 might participate in the subsequent reaction as a mild oxidant. Therefore, the presence of O_2 was also considered in this work to fully understand the DMP subsequent fate in AOPs. As shown in pathway (IV) of Figure 5, H-abstraction reaction by O_2 was an exothermic process with $\Delta G^{\ddagger}$ of 16.66 kcal mol^{-1}, and HOO• and *m*-OH-DMP would be the degradation products.

Fate of $^{\bullet}DMP(-H)\alpha$ Radical. The reaction pathways of $^{\bullet}DMP(-H)\alpha$ are depicted in SI Figure S8. $^{\bullet}DMP(-H)\alpha$ can be attacked by •OH to form the cation radical through the SET mechanism, pathway (V). Then MMP might be formed with loss of formaldehyde followed by further •OH addition, since the maximum $\Delta G^{\ddagger}$ of the pathway (V) is only 1.40 kcal mol^{-1}. However, $^{\bullet}DMP(-H)\alpha$ is prone to attack by •OH via a barrierless radical−radical reaction at −78.78 kcal mol^{-1} (pathway (VI)). This large released energy can completely overcome the energy barrier of 17.86 kcal mol^{-1} to produce MMP. Therefore, both pathways (V) and (VI) could be the feasible processes to form MMP.

In the presence of O_2, pathway (VII) of SI Figure S8, $^{\bullet}DMP(-H)\alpha$ could be directly attacked by O_2 to form the peroxyl radical (R−OO•). This pathway is a barrierless process with exothermic energy of −21.08 kcal mol^{-1}, followed by the reaction of the peroxyl radical (R−OO•) also with the release of energy, −69.53 kcal mol^{-1}. The highly exothermic sequence can completely overcome the final energy barrier of 28.95 kcal mol^{-1}, to produce MMP. Furthermore, MMP can undergo the similar HAT reaction with methyl group, leading to the formation of PA, which was confirmed by our experimental obtained data. The $\Delta G^{\ddagger}$ value of this pathway is 10.39 kcal mol^{-1}, 0.22 kcal mol^{-1} lower than that of the initial HAT_{α} step of DMP. The HAT reaction of MMP with •OH might be higher than that of DMP. That is, the initial reaction of DMP with •OH was likely the critical step during the degradation of DMP.

The goal of this work was to establish the underlying mechanisms involved in the •OH-mediated oxidation of an emerging contaminant (EC), dimethylphthalate. The implementation of AOPs in environmental applications requires an accurate prediction of the environmental fate and risk assessment of the target contaminants. To date, the direct detection of the reaction intermediates would be very challenging, partially because of the complexity of the reactions, as well as lack of authentic standards. Nevertheless, the quantum chemical calculation can provide a powerful tool to accurately predict the reaction pathways of contaminants remediated by •OH in AOPs, due to the excellent agreement with the experimental observations according to this study. These results were also very important to reveal the fate of ECs in water environments, since it is well-known that the ring-hydroxylated intermediates may cause more serious risk compared to parent compound.[53] As for ECs, the combined experimental and computational results of DMP suggested that besides the •OH addition to the aromatic ring, the HAT pathway at the methyl group might also represent an alternative mechanism to •OH-mediated reaction of DMP in aqueous

phase. Furthermore, the investigation is is underway to elucidate the structure-dependency of the reactive intermediates, as well as the quantitative evaluation of the health risk of the stable intermediates.

■ ASSOCIATED CONTENT

Supporting Information

Detailed descriptions of the mechanism calculation method of the single electron transfer reaction; the discussion on the reliability of the approaches; the parameters of the geometries, the simulated spectra are listed in Figures. This information is available free of charge via the Internet at http://pubs.acs.org.

■ AUTHOR INFORMATION

Corresponding Author

*Phone: +86-20-85291501 (T.A.); (574) 631-5411 (P.V.K.). Fax: +86-20-85290706 (T.A.); (574)631-8068 (P.V.K.). E-mail: antc99@gig.ac.cn (T.A.); pkamat@nd.edu (P.V.K.).

Notes

The authors declare no competing financial interest.

■ ACKNOWLEDGMENTS

This is Contribution No. IS-1521 from GIGCAS. The authors appreciate the financial support of the National Nature Science Foundation of China (40973068), Knowledge Innovation Program of CAS (KZCX2-YW-QN103), Sci. and Technol. R&D Fund of Shenzhen City (JC201005250054A), and earmarked Fund of SKLOG (SKLOG2011A02). T.A. also appreciates his award from the Chinese Scholarship Council for his visiting research in the U.S. The radiolysis experiments were carried out at Notre Dame Radiation laboratory, which is supported by the Division of Chemical Sciences, Geosciences, and Biosciences, Office of Basic Energy Sciences of the U.S. Department of Energy through Award DE-FC02-04ER15533. The analysis of the products was conducted at CEST, Univ. of Notre Dame. This contribution is NDRL 5000 from Notre Dame Radiation Laboratory.

■ REFERENCES

(1) An, T. C.; Yang, H.; Li, G. Y.; Song, W. H.; Cooper, W. J.; Nie, X. P. Kinetics and mechanism of advanced oxidation processes (AOPs) in degradation of ciprofloxacin in water. *Appl. Catal. B-Environ.* **2010**, *94* (3−4), 288−294, DOI: 10.1016/j.apcatb.2009.12.002.

(2) Bajt, O.; Mailhot, G.; Bolte, M. Degradation of dibutyl phthalate by homogeneous photocatalysis with Fe(III) in aqueous solution. *Appl. Catal. B-Environ.* **2001**, *33* (3), 239−248, DOI: 10.1016/S0926-3373(01)00179-5.

(3) Pignatello, J. J.; Oliveros, E.; MacKay, A. Advanced oxidation processes for organic contaminant destruction based on the Fenton reaction and related chemistry. *Crit. Rev. Environ. Sci. Technol.* **2006**, *36* (1), 1−84, DOI: 10.1080/10643380500326564.

(4) Konsowa, A. H.; Ossman, M. E.; Chen, Y. S.; Crittenden, J. C. Decolorization of industrial wastewater by ozonation followed by adsorption on activated carbon. *J. Hazard. Mater.* **2010**, *176* (1−3), 181−185, DOI: 10.1016/j.jhazmat.2009.11.010.

(5) Zhang, W. B.; An, T. C.; Xiao, X. M.; Fu, J. M.; Sheng, G. Y.; Cui, M. C. Photochemical degradation performance of quinoline aqueous solution in the presence of hydrogen peroxide. *J. Environ. Sci. Health, Part A: Toxic/Hazard. Subst. Environ. Eng.* **2003**, *38* (11), 2599−2611, DOI: 10.1081/Ese-120024442.

(6) Wu, M. H.; Liu, N.; Xu, G.; Ma, J.; Tang, L. A.; Wang, L. A.; Fu, H. Y. Kinetics and mechanisms studies on dimethyl phthalate degradation in aqueous solutions by pulse radiolysis and electron beam radiolysis. *Radiat. Phys. Chem.* **2011**, *80* (3), 420−425, DOI: 10.1016/j.radphyschem.2010.10.008.

(7) Yang, H.; Li, G. Y.; An, T. C.; Gao, Y. P.; Fu, J. M. Photocatalytic degradation kinetics and mechanism of environmental pharmaceuticals in aqueous suspension of TiO_2: A case of sulfa drugs. *Catal. Today* **2010**, *153* (3−4), 200−207, DOI: 10.1016/j.cattod.2010.02.068.

(8) Zhang, S. J.; Jiang, H.; Li, M. J.; Yu, H. Q.; Yin, H.; Li, Q. R. Kinetics and mechanisms of radiolytic degradation of nitrobenzene in aqueous solutions. *Environ. Sci. Technol.* **2007**, *41* (6), 1977−1982, DOI: 10.1021/Es062031l.

(9) An, T. C. Persistent organic pollutants in water and wastewater and their treatment by advanced oxidation processes. *Res. J. Chem. Environ.* **2007**, *11* (4), 3−4.

(10) Sun, W. J.; Yang, L. M.; Yu, L. Y.; Saeys, M. Ab initio reaction path analysis for the initial hydrogen abstraction from organic acids by hydroxyl radicals. *J. Phys. Chem. A* **2009**, *113* (27), 7852−7860, DOI: 10.1021/Jp8090792.

(11) Zhang, Q. Z.; Qu, X. H.; Wang, H.; Xu, F.; Shi, X. Y.; Wang, W. X. Mechanism and thermal rate constants for the complete series reactions of chlorophenols with H. *Environ. Sci. Technol.* **2009**, *43* (11), 4105−4112, DOI: 10.1021/Es9001778.

(12) Fang, H. S.; Gao, Y. P.; Li, G. Y.; An, J. B.; Wong, P. K.; Fu, H. Y.; Yao, S. D.; Nie, X. P.; An, T. C. Advanced oxidation kinetics and mechanism of preservative propylparaben degradation in aqueous suspension of TiO_2 and risk assessment of its degradation products. *Environ. Sci. Technol.* **2013**, *47* (6), 2704−2712, DOI: 10.1021/Es304898r.

(13) Chang, P. B. L.; Young, T. M. Kinetics of methyl *tert*-butyl ether degradation and by-product formation during UV/hydrogen peroxide water treatment. *Water Res.* **2000**, *34* (8), 2233−2240, DOI: 10.1016/S0043-1354(99)00392-9.

(14) Wardman, P. Reduction potentials of one-electron couples involving free-radicals in aqueous-solution. *J. Phys. Chem. Ref. Data* **1989**, *18* (4), 1637−1755.

(15) Naik, G. H.; Priyadarsini, K. I.; Maity, A. K.; Mohan, H. One electron oxidation induced dimerization of 5-hydroxytryptophol: Role of 5-hydroxy substitution. *J. Phys. Chem. A* **2005**, *109* (10), 2062−2068, DOI: 10.1021/Jp048157r.

(16) Galano, A.; Alvarez-Idaboy, J. R. Guanosine plus OH radical reaction in aqueous solution: A reinterpretation of the UV-vis data based on thermodynamic and kinetic calculation. *Org. Lett.* **2009**, *11* (22), 5114−5117, DOI: 10.1021/Ol901862h.

(17) Mohan, H.; Mittal, J. P. Pulse radiolysis investigations on acidic aqueous solutions of benzene: Formation of radical cations. *J. Phys. Chem. A* **1999**, *103* (3), 379−383, DOI: 10.1021/Jp983255w.

(18) Geeta, S.; Rao, B. S. M.; Mohan, H.; Mittal, J. P. Radiation-induced oxidation of substituted benzaidehydes: A pulse radiolysis study. *J. Phys. Org. Chem.* **2004**, *17* (3), 194−198, DOI: 10.1002/poc.713.

(19) Nicolaescu, A. R.; Wiest, O.; Kamat, P. V. Radical-induced oxidative transformation of quinoline. *J. Phys. Chem. A* **2003**, *107* (3), 427−433, DOI: 10.1021/jp027112s.

(20) Mezyk, S. P.; Neubauer, T. J.; Cooper, W. J.; Peller, J. R. Free-radical-induced oxidative and reductive degradation of sulfa drugs in water: Absolute kinetics and efficiencies of hydroxyl radical and hydrated electron reactions. *J. Phys. Chem. A* **2007**, *111* (37), 9019−9024, DOI: 10.1021/jp073990k.

(21) Sehested, K.; Christensen, H. C.; Hart, E. J.; Corfitzen, H. Rates of reaction of O-, OH, and H with methylated benzenes in aqueous solution-optical-spectra of radicals. *J. Phys. Chem.* **1975**, *79* (4), 310−315, DOI: 10.1021/j100571a005.

(22) Song, W. H.; Xu, T. L.; Cooper, W. J.; Dionysiou, D. D.; De La Cruz, A. A.; O'Shea, K. E. Radiolysis studies on the destruction of microcystin-LR in aqueous solution by hydroxyl radicals. *Environ. Sci. Technol.* **2009**, *43* (5), 1487−1492, DOI: 10.1021/es802282n.

(23) Alam, M. S.; Rao, B. S. M.; Mohan, H.; Mittal, J. P. Study of radiation chemical reactions of oxidising and reducing radicals with furazan derivatives. *J. Photochem. Photobiol., A* **2001**, *143* (2−3), 181−189, DOI: 10.1016/S1010-6030(01)00529-9.

(24) Rao, P. S.; Hayon, E. Oxidation of aromatic-amines and diamines by OH radicals—Formation and ionization-constants of

amine cation radicals in water. *J. Phys. Chem.* **1975**, *79* (11), 1063−1066, DOI: 10.1021/j100578a005.
(25) Tripathi, G. N. R. Electron-transfer component in hydroxyl radical reactions observed by time resolved resonance Raman spectroscopy. *J. Am. Chem. Soc.* **1998**, *120* (17), 4161−4166, DOI: 10.1021/Ja9800838.
(26) Tripathi, G. N. R.; Sun, Q. Time-resolved Raman study of the oxidation mechanism of aromatic diamines by (OH)−O-center dot radical in water. *J. Phys. Chem. A* **1999**, *103* (45), 9055−9060, DOI: 10.1021/Jp9927552.
(27) Minakata, D.; Crittenden, J. Linear free energy relationships between aqueous phase hydroxyl radical reaction rate constants and free energy of activation. *Environ. Sci. Technol.* **2011**, *45* (8), 3479−3486, DOI: 10.1021/Es1020313.
(28) Minakata, D.; Song, W. H.; Crittenden, J. Reactivity of aqueous phase hydroxyl radical with halogenated carboxylate anions: Experimental and theoretical studies. *Environ. Sci. Technol.* **2011**, *45* (14), 6057−6065, DOI: 10.1021/Es200978f.
(29) Nicolaescu, A. R.; Wiest, O.; Kamat, P. V. Mechanistic pathways of the hydroxyl radical reactions of quinoline. 2. Computational analysis of hydroxyl radical attack at C atoms. *J. Phys. Chem. A* **2005**, *109* (12), 2829−2835, DOI: 10.1021/jp045016g.
(30) Giam, C. S.; Chan, H. S.; Neff, G. S.; Atlas, E. L. Phthalate ester plasticizers—New class of marine pollutant. *Science* **1978**, *199* (4327), 419−421, DOI: 10.1126/science.199.4327.419-a.
(31) Koniecki, D.; Wang, R.; Moody, R. P.; Zhu, J. P. Phthalates in cosmetic and personal care products: Concentrations and possible dermal exposure. *Environ. Res.* **2011**, *111* (3), 329−336, DOI: 10.1016/j.envres.2011.01.013.
(32) Buxton, G. V.; Stuart, C. R. Reevaluation of the thiocyanate dosimeter for pulse-radiolysis. *J. Chem. Soc., Faraday Trans.* **1995**, *91* (2), 279−281, DOI: 10.1039/Ft9959100279.
(33) Buxton, G. V.; Greenstock, C. L.; Helman, W. P.; Ross, A. B. Critical-review of rate constants for reactions of hydrated electrons, hydrogen-atoms and hydroxyl radicals ($^{\bullet}OH/^{\bullet}O^{-}$) in aqueous-solution. *J. Phys. Chem. Ref. Data* **1988**, *17* (2), 513−886.
(34) Song, W.; Cooper, W. J.; Mezyk, S. P.; Greaves, J.; Peake, B. M. Free radical destruction of beta-blockers in aqueous solution. *Environ. Sci. Technol.* **2008**, *42* (4), 1256−1261, DOI: 10.1021/Es702245n.
(35) Frisch, M. J.; Truck, G. W.; Schlegel, H. B.; Scuseria, G. E.; Robb, M. A.; Cheeseman, J. R.; Zakrzewski, V. G.; Montgomery, J. A.; Stratmann, J. R. E.; Burant, J. C.; Dapprich, S.; Millam, J. M.; Daniels, A. D.; Kudin, K. N.; Strain, M. C.; Farkas, O.; Tomasi, J.; Barone, V.; Cossi, M.; Cammi, R.; Mennucci, B.; Pomelli, C.; Adamo, C.; Clifford, S.; Ochterski, J.; Petersson, G. A.; Ayala, P. Y.; Cui, Q.; Morokuma, K.; Malick, D. K.; Rabuck, A. D.; Raghavachari, K.; Foresman, J. B.; Cioslowski, J.; Ortiz, J. V.; Boboul, A. G.; Stefnov, B. B.; Liu, G.; Liaschenko, A.; Piskorz, P.; Komaromi, L.; Gomperts, R.; Martin, R. L.; Fox, D. J.; Keith, T.; Al−Laham, M. A.; Peng, C. Y.; Nanayakkara, A.; Gonzalez, C.; Challacombe, M.; Gill, P. M. W.; Johnson, B.; Chen, W.; Wong, M. W.; Andres, J. L.; Gonzalez, C.; Head−Gordon, M.; Replogle, E. S.; Pople, J. A. Gaussian 03; Guassian, Inc.: Pittsburgh, PA, 2003.
(36) Barone, V.; Cossi, M. Quantum calculation of molecular energies and energy gradients in solution by a conductor solvent model. *J. Phys. Chem. A* **1998**, *102* (11), 1995−2001, DOI: 10.1021/jp9716997.
(37) Tomasi, J.; Mennucci, B.; Cammi, R. Quantum mechanical continuum solvation models. *Chem. Rev.* **2005**, *105* (8), 2999−3093, DOI: 10.1021/Cr9904009.
(38) An, T. C.; Yang, H.; Song, W. H.; Li, G. Y.; Luo, H. Y.; Cooper, W. J. Mechanistic considerations for the advanced oxidation treatment of fluoroquinolone pharmaceutical compounds using TiO_2 heterogeneous catalysis. *J. Phys. Chem. A* **2010**, *114* (7), 2569−2575, DOI: 10.1021/Jp911349y.
(39) Steenken, S.; Ramaraj, R. Comparison of reactions of radical cations of 1-phenylalkanols produced by photoionization and by one-electron oxidation in aqueous solution. *J. Chem. Soc., Perkin Trans.* **2001**, *9*, 1613−1619, DOI: 10.1039/B102515p.
(40) Mezyk, S. P.; Jones, J.; Cooper, W. J.; Tobien, T.; Nickelsen, M. G.; Adams, J. W.; O'Shea, K. E.; Bartels, D. M.; Wishart, J. F.; Tornatore, P. M.; Newman, K. S.; Gregoire, K.; Weidman, D. J. Radiation chemistry of methyl *tert*-butyl ether in aqueous solution. *Environ. Sci. Technol.* **2004**, *38* (14), 3994−4001, DOI: 10.1021/es034558t.
(41) Wen, G.; Ma, J.; Liu, Z. Q.; Zhao, L. Ozonation kinetics for the degradation of phthalate esters in water and the reduction of toxicity in the process of O_3/H_2O_2. *J. Hazard. Mater.* **2011**, *195*, 371−377, DOI: 10.1016/j.jhazmat.2011.08.054.
(42) Xu, B.; Gao, N. Y.; Cheng, H. F.; Xia, S. J.; Rui, M.; Zhao, D. D. Oxidative degradation of dimethyl phthalate (DMP) by UV/H_2O_2 process. *J. Hazard. Mater.* **2009**, *162* (2−3), 954−959, DOI: 10.1016/j.jhazmat.2008.05.122.
(43) Alfassi, Z. B.; Prutz, W. A.; Schuler, R. H. Intermediates in the oxidation of azide ion in acidic solutions. *J. Phys. Chem.* **1986**, *90* (6), 1198−1203, DOI: 10.1021/J100278a047.
(44) Hayon, E.; Simic, M. Absorption spectra and kinetics of the intermediate produced from the decay of azide radicals. *J. Am. Chem. Soc.* **1970**, *92* (25), 7486−7487, DOI: 10.1021/ja00728a049.
(45) Alfassi, Z. B.; Schuler, R. H. Reaction of azide radicals with aromatic compounds. Azide as a selective oxidant. *J. Phys. Chem.* **1985**, *89* (15), 3359−3363, DOI: 10.1021/j100261a040.
(46) Ram, M. S.; Stanbury, D. M. Reduction potential of the trinitrogen radical as determined by chemical-kinetics—Novel application of spin trapping. *Inorg. Chem.* **1985**, *24* (25), 4233−4234, DOI: 10.1021/Ic00219a004.
(47) Huie, R. E.; Clifton, C. L.; Neta, P. Electron-transfer reaction-rates and equilibria of the carbonate and sulfate radical-anions. *Radiat. Phys. Chem.* **1991**, *38* (5), 477−481.
(48) Neta, P.; Madhavan, V.; Zemel, H.; Fessenden, R. W. Rate constants and mechanism of reaction of sulfate radical anion with aromatic compounds. *J. Am. Chem. Soc.* **1977**, *99* (1), 163−164, DOI: 10.1021/ja00443a030.
(49) Zemel, H.; Fessenden, R. W. The mechanism of reaction of sulfate radical anion with some derivatives of benzoic acid. *J. Phys. Chem.* **1978**, *82* (25), 2670−2676, DOI: 10.1021/j100514a008.
(50) Al-Sheikhly, M.; Poster, D. L.; An, J. C.; Neta, P.; Silverman, J.; Huie, R. E. Ionizing radiation-induced destruction of benzene and dienes in aqueous media. *Environ. Sci. Technol.* **2006**, *40* (9), 3082−3088, DOI: 10.1021/es052533j.
(51) An, T. C.; Li, G. Y.; Zhu, X. H.; Fu, J. M.; Sheng, G. Y.; Zhu, Z. Photoelectrocatalytic degradation of oxalic acid in aqueous phase with a novel three-dimensional electrode-hollow quartz tube photo-electrocatalytic reactor. *Appl. Catal., A* **2005**, *279* (1−2), 247−256, DOI: 10.1016/j.apcata.2004.10.033.
(52) Duesteberg, C. K.; Waite, T. D. Kinetic modeling of the oxidation of *p*-hydroxybenzoic acid by Fenton's reagent: Implications of the role of quinones in the redox cycling of iron. *Environ. Sci. Technol.* **2007**, *41* (11), 4103−4110, DOI: 10.1021/es0628699.
(53) Kusu, R.; Toda, C.; Okamoto, Y.; Tozuka, Y.; Ueda, K.; Kojima, N. Structural properties of estrogen receptor ligand obtained by study of hydroxylated phthalate ester derivatives. *Environ. Toxicol. Pharmacol.* **2007**, *24* (3), 311−315, DOI: 10.1016/j.etap.2007.08.002.